STEM CELLS AND DEVELOPMENT
Volume 23, Number 14, 2014

DOI: 10.1089/scd.2013.0645

Cationic Surface Charge Combined with Either Vitronectin or Laminin Dictates the Evolution of Human Embryonic Stem Cells/Microcarrier Aggregates and Cell Growth in Agitated Cultures

Alan Tin-Lun Lam,[1] Jian Li,[2] Allen Kuan-Liang Chen,[1] Shaul Reuveny,[1] Steve Kah-Weng Oh,[1] and William R. Birch[2]

The expansion of human pluripotent stem cells (hPSC) for biomedical applications generally compels a defined, reliable, and scalable platform. Bioreactors offer a three-dimensional culture environment that relies on the implementation of microcarriers (MC), as supports for cell anchorage and their subsequent growth. Polystyrene microspheres/MC coated with adhesion-promoting extracellular matrix (ECM) protein, vitronectin (VN), or laminin (LN) have been shown to support hPSC expansion in a static environment. However, they are insufficient to promote human embryonic stem cells (hESC) seeding and their expansion in an agitated environment. The present study describes an innovative technology, consisting of a cationic charge that underlies the ECM coatings. By combining poly-L-lysine (PLL) with a coating of ECM protein, cell attachment efficiency and cell spreading are improved, thus enabling seeding under agitation in a serum-free medium. This coating combination also critically enables the subsequent formation and evolution of hPSC/MC aggregates, which ensure cell viability and generate high yields. Aggregate dimensions of at least 300 μm during early cell growth give rise to ≈ 15-fold expansion at 7 days' culture. Increasing aggregate numbers at a quasi-constant size of ≈300 μm indicates hESC growth within a self-regulating microenvironment. PLL + LN enables cell seeding and aggregate evolution under constant agitation, whereas PLL + VN requires an intermediate 2-day static pause to attain comparable aggregate sizes and correspondingly high expansion yields. The cells' highly reproducible bioresponse to these defined and characterized MC surface properties is universal across multiple cell lines, thus confirming the robustness of this scalable expansion process in a defined environment.

Introduction

Human pluripotent stem cells (hPSC), which encompass human embryonic stem cells (hESC) isolated from the inner cell mass of the blastocyst and human-induced pluripotent stem cells (hiPSC), have been the object of extensive exploration for their potential to differentiate into the cell lineages that compose functional tissues, such as the heart, retina, ear cartilage, platelets, neurons, and pancreatic cells [1–8]. Clinical applications and biotechnological drug-screening purposes require significant quantities of these cells, generated in a reliable, reproducible, and defined environment. Scalable systems offer an enabling technology that meets this demand through the industrial-scale production of hPSC. A primary means toward this goal are microcarrier (MC)-based, three-dimensional (3D) culture environments for hPSC expansion in a bioreactor, under stirring or agitation [9,10]. This technology presents the advantage of a high surface-to-volume ratio, the opportunity to monitor and control culture parameters, and the possibility of its efficient scale up [11]. Several reports of extracellular matrix (ECM)-coated commercial MC as viable supports for hPSC expansion implement nondefined coatings [7,10,12–15], rely on serum-containing cell culture media [16,17], and use static cultures [18,19], which are not suitable for scalable production in bioreactors. Although these environments satisfactorily expand hPSC, the large hPSC/MC aggregates formed in static culture yield low cell-fold expansion. This may be due to a diffusional limitation, as compared with the smaller aggregates formed in agitated conditions, which generate significantly higher cell-fold expansion [9]. A recent report of static hESC expansion on MC coated with defined ECM proteins, vitronectin (VN), and laminin (LN) in a defined medium achieved 8.5 cell-fold expansion, without loss

[1]Stem Cell Group, Bioprocessing Technology Institute, Agency for Science, Technology and Research (A*STAR), Singapore, Singapore.
[2]Institute of Materials Research and Engineering, Agency for Science, Technology and Research (A*STAR), Singapore, Singapore.

of pluripotent marker expression [18]. The present study capitalizes on this first report of a defined 3D environment by exploring the required MC surface properties for transposing this culture into an environment either under agitation or in stirred spinner flasks, which are a model for the scalable expansion of hPSC in bioreactors.

Anchorage-dependent hESC expansion relies on coating the solid support with adhesion-promoting ECM proteins, which include LN, VN, fibronectin, and collagen [11,14,18]. LN is a basement membrane glycoprotein, known to mediate cell adhesion, differentiation, migration, and phenotype stability [20,21]. This heterotrimer exists in a variety of isoforms, assembled from α, β, and γ chain subunits [22], which are ubiquitous in the ECM [20,23]. Polystyrene (PS) substrates coated with murine LN111, extracted from an Engelbreth-Holm-Swarm sarcoma [18,24,25], promote hESC adhesion and support their long-term expansion in planar, 2D cultures. PS substrates coated with human LN511 [20,26,27] or recombinant E8 fragments of LN511 [28] and LN521 [20,24] also support hESC expansion. VN exhibits a significantly different structure. This multifunctional monomeric glycoprotein, which is found in both plasma and the ECM [29], adsorbs to surfaces [30]. PS substrates coated with VN promote hESC attachment [20,31] and support their long-term expansion [31–34], exhibiting performance on par with LN and Matrigel [18,31–34].

Stirring and agitation generate shear gradients that may lead to collisions of MC with each other and the walls of the vessel [12,35,36]. These hydrodynamic forces and impacts induce stresses that can adversely affect cell attachment, spreading, and growth. They are also known to compromise cell viability [37–40] and may induce the premature and undesired differentiation of hPSC [9,41]. Despite their potential for compromising scalable processes in bioreactors [9,25], a few studies have explored the effect that hydrodynamic forces have on hPSC expansion and their evolution. The present study elucidates requirements for MC-based hPSC expansion that can be implemented in agitated and stirred culture environments, as required by scalable 3D bioreactors. It addresses how defined MC surface properties, such as surface charge and coatings, regulate hPSC attachment, spreading, and migration. Most importantly, it reveals the critical parameters that affect the evolution of hPSC/MC aggregates, which, ultimately, determine hPSC expansion efficiency.

Materials and Methods

Cells

hESC lines HES-3 (ES Cell International) and H7 (WiCell Research Institute, Inc.), and the induced pluripotent stem cell line IMR90 (generously provided by James Thomson [42]), were routinely maintained on Matrigel-coated tissue culture plates with mTeSR™1 medium (05850; StemCell Technologies), as described in previous articles [9,43].

Matrices and coating MC with poly-L-lysine, LN, and VN

PS microspheres/MC with an average diameter of $97 \pm 10\,\mu m$ were purchased from Thermo-Fisher Scientific (#7602B). Cytodex 1 (17-0448-01; GE HealthCare) served as a positive cell attachment control. Poly-L-lysine (PLL, P6282; Sigma), with a molecular weight of 70–150 kDa, human plasma-purified VN (CC080; Millipore) >90% purity, and natural mouse LN from the Engelbreth-Holm-Swam sarcoma (LN, 23017-015; Invitrogen) >95% purity were used to coat the PS MC [18,25,34]. PS MC were coated in phosphate-buffered saline (PBS), following the procedures described in Heng et al. [18]. The PLL coating was applied by adding 12 μL of 1 mg/mL of PLL to 20 mg of MC in 600 μL PBS solution, to make a final PLL concentration of 20 μg/mL, which was incubated at 4°C under agitation and, subsequently, rinsed thrice in PBS before use. ECM protein coatings were similarly applied: 12 or 20 μL of 1 mg/mL of VN or LN, respectively, was added to 20 mg of either bare or PLL-coated MC in 600 μL PBS, to make final VN and LN protein concentrations of 20 and 33 μg/mL, respectively. These were incubated at 4°C overnight, followed by rinsing thrice in PBS before use.

Surface characterization

Surface-adsorbed VN and LN were quantified by their depletion from the depositing solution, whose concentration was quantified by a modified Bradford assay [44], as described in Heng et al. [18]. Briefly, 0, 5, 10, 20, 30, and 40 μg/mL of VN or LN in 600 μL PBS were incubated overnight with 20 mg MC + PLL in a 24-well plate at 4°C. The residual protein concentrations in the supernatants were quantified using the Bradford protein assay (500-001; Bio-Rad). Ponceau S (P7170; Sigma) stain was used to distinguish protein adsorbed on the surface of the well from that adsorbed on the MC, as described by Heng et al. [18]. The adsorbed Ponceau S stain enabled a calculation of the ratio of protein adsorbed to the container versus that adsorbed to MC, for VN and LN, respectively, at each concentration. This ratio was used to calculate the surface density of adsorbed VN or LN, respectively, using the depletion of protein from the depositing solution and based on an area of 11 cm^2 for 20 mg of MC.

Measurement of Zeta potential and pKa

The electrical double layer of bare and coated MC was probed by the Zeta potential. A ZetaPlus Analyzer (Brookhaven Instruments) used phase analysis light scattering, with palladium electrodes and an He-Ne laser light source, to measure the Zeta potential in deionized water. The apparent acid dissociation constant ($pK_{a,\,app}$) was quantified by pH titration. Fifty milligrams of PLL-coated MC were rinsed twice in 0.1 M aqueous NaCl solution and dispersed into a polypropylene beaker (AZLON®) containing 10 mL of the same solution. The $pK_{a,\,app}$ of PLL-coated MC was then titrated with 0.02 M aqueous NaOH solution using a pH meter (5-Star; Orion). The same titration procedure for 6.25 mg of dry Cytodex 1 dispersed in 10 mL of 0.1 M aqueous NaCl solution measured the $pK_{a,\,app}$ of these MC, with a surface area equivalent to that of 50 mg PS MC.

Cell attachment and spreading

Cell aggregates were dissociated with TrypLE™ Express (12604-013; Invitrogen). Viable cells in a single-cell suspension (2×10^5 cells/mL for the attachment test and 0.4×10^5 cells/mL for the spreading test) were then seeded onto MC (20 mg for the attachment test and 5 mg for the

spreading test) in two 6-well ultra-low attachment plates (Corning 3471) containing 5 mL of mTeSR1 medium. The seeding ratio for the Cytodex 1 (positive control) and PS MC was kept constant at 100,000 cells/cm^2 for the attachment test. Cells added to the MC at zero time were allowed to attach and spread over a period of 2 h. For agitated cultures, one of the plates was agitated for 2 h on an orbital shaker (KS260 control; IKA), at 110 rpm, in an incubator set to 37°C and 5% CO_2. For static cultures, the second plate was placed in the same incubator without any shaking. The attachment assay consisted of using a NucleoCounter (NC-3000; ChemoMetec) to quantify nuclei counts, after acridine orange and DAPI staining, of viable unattached cells in aliquots of supernatants, which were taken at the following times: 10, 20, 30, 60, and 120 min. The attachment efficiency was calculated by subtracting the concentration of unattached cells from the initial viable cell concentration. Attachment kinetics, inferred from the rate of decrease in unattached cells after cell seeding, were modeled using an exponential decay of the form $C_t = C_0\, e^{-kt}$ [45], where C_t is the concentration of unattached cells at time t, C_0 is the original cell concentration, and k is the rate constant. This equation was expressed logarithmically as $-\ln (C_t/C_0) = kt$, which defines the specific attachment rate, k, in cells per cm^2, per min.

The cell spreading efficiency was determined by phase-contrast microscopy (IX70; Olympus) imaging of individual cells attached to MC. The ratio of the length (L) of the cell base and its height (H) (see Fig. 3) was measured for more than 20 spreading cells (each attached to a separate MC). This ratio represents the extent of spreading, where rounded cells yield a value of ≈ 1 and fully spread and flattened cells yield ≈ 5.

Cell growth

A single-cell suspension containing 1×10^6 cells (HES-3, HES-7, or IMR90, respectively) was used to seed coated MC in the wells of a six-well ultra-low attachment plate. The plate was then placed on an orbital shaker at 110 rpm in a 37°C/5% CO_2 incubator for 2 h to enable seeding of hESC onto MC [18,25]. Cells were then cultured for 7 days under different agitation regimes: (1) 7 days of static pause (0 day agitation), (2) 2 days of static pause followed by 5 days of agitation (2 days static), (3) 1 day of static pause followed by 6 days of agitation (1 day static), and (4) 7 days of agitation (continuous agitation). The Nucleocounter, as described earlier, was used to determine cell concentration and viability at day 7. Fold expansion was calculated by dividing the cell density at day 7 by the inoculum's cell density at day 0.

Number of free MC, hESC/MC aggregates, and their corresponding size

Twenty or more phase-contrast microscopy (IX70; Olympus) images of random areas (each containing at least 10 hESC/MC aggregates in the field of view) were taken of each MC culture, except LN-coated MC, at days 0, 1, 2, 3, 5, and 7. These images were processed with Olympus DP2-DSW displaying software, and the linear dimensions of the hESC/MC aggregates were estimated by calculating the square root of their area, using NIH ImageJ software. The number density of aggregates and the number of free MC were similarly counted on each image using the automatic cell counter plug-in of ImageJ. The percentage of free MC was defined as (free MC)/(seeded MC) × 100, with an estimate of ≈ 40,000 MC per 20 mg mass.

Cell entrapment

One hESC/MC aggregate, obtained from cell cultures at 5–6 days of MC coated with VN, LN, PLL + VN, and PLL + LN (from their 2 days' static, 1 day static, 2 days' static, and continuous agitated cultures, respectively), and five single MCs were transferred into a well of a 96-well ultra-low attachment plate (3474; Corning). This was placed in the incubation chamber of a Nikon Eclipse Ti microscope (Nikon Instruments, Inc.), where it was continuously video recorded by NIS Elements 4.10.00 software (Nikon Instruments, Inc.) over 24 h. For a free MC coming into contact with an hESC/MC aggregate, the first contact was taken as time zero (Fig. 7: time = 0) and measurement was continued until either 24 h elapsed or it was completely covered by a layer of cells. The latter time was averaged over five aggregates.

Spinner flask cultures

Mechanically dissociated HES-3 cells, obtained from cultures of MC coated with PLL + VN (2 days static) or PLL + LN (continuous agitation), were seeded at a density of 2×10^5 cells/mL into a presiliconized (Sigmacote, SL2-25ML; Sigma) 100-mL spinner flask (1965-00100; Bellco) containing 25 mL of mTeSR1 medium and 4 mg/mL of MC coated with PLL + VN or PLL + LN, respectively. The culture was incubated at 37°C/5% CO_2 under static conditions for 2 or 1 day, for PLL + VN or PLL + LN, respectively. After a top up of the medium to 50 mL, the culture was agitated at 25 rpm, for 7 or 8 days, for PLL + VN or PLL + LN, respectively. Eighty percent of spent medium was removed daily and replaced with fresh mTeSR1 medium. Cell concentration and viability were monitored daily and pluripotent markers were measured on day 9, using the NC-3000 Nucleocounter, as described earlier.

Fluorescence-activated cell sorting analysis

Flow cytometry analysis was performed with the extracellular antigens Tra-1-60 (MAB4360; Millipore) and mAb84 [46], and intracellular transcription factor Oct-4 (sc-8628; Santa Cruz). Cells were first trypsinized with TrypLE Express to a single-cell suspension and then filtered through a 40-μm sieve (352340; BD Biosciences) to remove cells debris and MC. They were then fixed and permeabilized with a Fix and Perm Cell Permeabilization reagent kit (GAS003; Invitrogen), which was used according to the manufacturer's instructions. During the 15 min permeabilization step, mouse primary antibodies Tra-1-60 (1:50), Oct-4 (1:20), and mAb84 (1:20) were incubated along with the kit's Reagent B. The cells were then washed in 1% bovine serum albumin (BSA)/PBS, followed by a 15 min incubation in the dark with a 1:500 dilution of goat anti-mouse antibody FITC-conjugated (Z0420; DAKO). Finally, they were again washed and resuspended with 1% BSA/PBS for analysis on an FACSCalibur (Becton-Dickinson). Results

were analyzed with FlowJo (Tree Star), with gating selected at the point of intersection between the marker and its isotype control [14,47].

In vitro differentiation

Spontaneous in vitro differentiation was carried out with embryoid bodies (EB) to determine whether HES-3 cells cultured on either PLL + LN or PLL + VN-coated MC retain their ability to differentiate into the three primary germ layers. Briefly, after expansion in spinner flask cultures, hESC/MC aggregates were cultured for 7 days in differentiation medium [Knockout™ DMEM (12660-012; Invitrogen) with 15% FBS (160000-44; Invitrogen)] on nonadherent dishes (3737; Corning). The cells were subsequently re-plated on 0.1% gelatinized plates and cultured for another 14 days at 37°C/5% CO_2 in an incubator. Immunostaining of the differentiated cells was carried out with α-smooth muscle actin, SMA (A2547; Sigma), β-III tubulin (AB9354; Millipore), and α-fetoprotein, AFP (A8452; Sigma), as previously described. The cells were then fixed, using 4% paraformaldehyde (v/v) for 15 min, and then blocked for 2 h in PBS containing 0.1% Triton X-100, 10% goat serum, and 1% BSA. They were probed with primary antibodies against SMA (1:400), β-III tubulin (1:1,000), and AFP (1:250) for 1 h and secondary FITC-conjugated antibody (A11001; Invitrogen) for another 2 h at room temperature. A fluorescent mounting medium with DAPI (H-1200; Vectashield) was added to cover the cells, and it was incubated for 1 h before imaging with a fluorescence microscope (Axiovert 200M; Carl Zeiss) [18,25].

Quantitative real-time PCR

Quantitative real-time PCR (qPCR) was carried out following the procedure described by Heng et al. [18]. RNA extracted from undifferentiated and differentiated cells, using an RNA extraction kit (RNeasy Mini Kit, 74106; Qiagen) in accordance with the manufacturer's instructions, was compared with RNA that was harvested from undifferentiated HES-3 cells. The purity and concentration of RNA were quantified using a Nanodrop Spectrophotometer (ND-1000; Thermo Scientific). RNA was reverse transcribed into cDNA using Superscript II Reverse Transcriptase (11904-018; Invitrogen). cDNA was mixed with *Power* SYBR® Green PCR Master Mix (Life technologies 4367659) and 200 nM of specific primers of the following genes, *OCT-4*, *NANOG*, *AFP*, *GATA6*, *Hand1*, *Nkx2.5*, *PAX6*, *SOX1*, and *GAPDH* (housekeeping gene), as described by Chen et al. [25]. The qPCR reaction was carried on an ABI Prism® 7500 Real-Time PCR system (Applied Biosystems) using the following cycles: 50°C for 2 min, 95°C for 10 min, followed by 40 cycles of 95°C for 15 s and 60°C for 1 min. Data analysis referenced the fold change of each gene to the same before HES-3 differentiation.

Induction of CM differentiation

To induce the differentiation of expanded hESC into cardiac cells, a modified version of the two Wnt signaling inhibitors method was used [48]. After their expansion in spinner flask cultures by MC coated with PLL + LN, 1×10^6 HES-3 cells were replated in six-well plates, which were formerly coated from 10 μg/mL LN solution. The cells were treated with 12 μM Gsk3 inhibitor CHIR99021 (CT-99021; Selleck) in RPMI/B27 without insulin (RPMI-1640, 11875-119; B27® supplement minus insulin, 0050129-SA; Invitrogen) for 24 h (day 0 to 1). The medium was changed to RPMI/B27 without insulin, which was followed at day 3 by treatment with 5 μM inhibitor of Wnt production-2 (IWP2, 04-0034; Stemgent). This was replaced on day 5 by fresh PRMI/B27 without insulin and cells were maintained in this medium until day 10, when they were again maintained in RPMI/B27 with insulin (B27® Supplement, 0080085-SA) until day 15. The cells were then trypsinized into a single-cell suspension and fixed with a Fix and Perm Cell Permeabilization reagent kit, as described earlier. Cells were stained with 5:200 anti-Cardiac myosin heavy chain (MF20; Developmental Studies Hybridoma Bank) and 1:200 anti-troponin T cardiac (cTnT, CB1027; Millipore) before fluorescence-activated cell sorting analysis, as described earlier.

Statistical analysis

All experiments were run in duplicate, and they were repeated twice or thrice. All data are presented as mean ± standard deviations, unless stated otherwise. Statistical significance of differences was calculated using Student's *t*-test. Significance was accepted at two levels: $*P < 0.05$ and $**P < 0.01$.

Results and Discussion

The quest for a defined environment for hESC propagation led to tissue culture PS plates, coated with either VN or LN, being demonstrated as capable of supporting the long-term expansion of cells and exhibiting a performance on par with Matrigel™ [33,34]. These cell culture substrate coatings were successfully transposed from planar surfaces onto 3D MC, yielding the first MC-based hESC culture in a defined environment [18]. In order to pursue these promising results, subsequent exploration focused on implementing PS MC coated with adhesion-promoting ECM proteins in a stirred culture environment.

Establishing hESC/MC culture in a stirred or agitated environment relies on promoting cell attachment, their spreading, and the subsequent formation of hESC/MC aggregates. The first step targets single hESC adhesion onto the MC surface within 1–2 h, with a high degree of efficiency. This initial cell seeding, which is critical to the success of this process, needs to occur in the presence of hydrodynamic forces that are generated by agitation [30]. Delayed cell attachment generally leads to cell death and can induce the development of differentiating EB [25]. During subsequent hours, attached hESC flatten and extensively deform their shape as they spread on the MC [17,49]. Binding interactions between endogenous integrins, found in the hESC membrane, and exogenous ECM protein, presented at the MC surface, lead to a cascade of signaling events. This results in cytoskeleton assembly and the subsequent initiation of cell division [30]. With shear gradients and putative MC collisions known to affect cell spreading [35,36,40,50], MC surface properties that generate sufficiently robust cell attachment and engender their efficient spreading in agitated cultures represent a critical enabling technology for efficient cell growth under agitation.

Initial cell seeding is followed by the formation of hESC/MC aggregates, within which hESC propagate and may attain several-fold expansion [18,25]. The MC surface properties required for the formation and evolution of these aggregates are key to achieving high cell yields over several days' culture in scalable bioreactors.

MC characterization

Spherical PS MC with a diameter of $93 \pm 10\,\mu m$ were used as cell culture supports. Figure 1 presents the characterization of their surface properties, bare, coated with cationic polyelectrolyte (PLL), and VN or LN, respectively. The negative surface charge presented by bare MC adsorbs PLL, attaining a saturation surface density of $150\,ng/cm^2$ when deposited from concentrations higher than $5\,\mu g/mL$ PLL. Measurements of surface staining and PLL surface density, inferred from depletion of the depositing solution concentration, are shown in Fig. 1A and B, respectively.

Adsorption of ECM protein onto bare or PLL-coated MC generates similar isotherms, which are distinct for VN and LN. As in previous reports [18,34], VN surface density saturates at $\sim 500\,ng/cm^2$; while LN surface density attains surface densities approaching $700\,ng/cm^2$ (Fig. 1D). These surface densities correspond to a quasi-monolayer coverage of adsorbed protein molecules [18]. Similar trends are discerned with ECM protein surface staining (Fig. 1C) and by surface density quantification, inferred from depletion of the depositing solution concentration (Fig. 1D). Higher Ponceau S staining reflects a greater affinity for VN, as compared with LN (Fig. 1C). MC used for cell cultures were coated with VN and LN surface densities approaching their saturation values, deposited from solution concentrations $\geq 20\,\mu g/mL$.

Zeta potential measurements, shown in Fig. 1E, reflect the extent of the diffuse electrical double layer, thus providing an indication of the exposed surface charge. The value of $-80\,mV$ potential generated by bare MC is gradually neutralized and then overcompensated by adsorbed PLL, which yields approximately $\pm 80\,mV$ at saturation surface density. In comparison, Cytodex 1 MC has a zeta potential of $+40\,mV$. The adsorption of VN or LN, respectively, appears to progressively neutralize the MC surface charge. An exception is LN, which is discussed later, in relation to MC aggregation before contact with hESC. Interestingly, the evolution of Zeta potential for VN or LN adsorbed onto PLL-coated bare MC follows a similar trend to the adsorption isotherms (Fig. 1C, D); while their adsorption on bare PLL-coated MC exhibits a slower progressive neutralization of the Zeta potential.

Measuring $pK_{a,\ app}$ values (Fig. 1F) probes the PLL coating's effectiveness to adsorb hydroxyl ions. These data follow a trend matching the adsorption isotherms (Fig. 1A, B) and Zeta potential measurements (Fig. 1E). From Ponceau S stain, a rough estimation of the surface charge of PLL-coated MC is $2\text{–}4 \times 10^{-4}$ meq/g. Cytodex 1 are charged throughout their volume, with a manufacturer-specified charge of 1.2–1.6 meq/g dry weight, corresponding to 24–32 meq/g for the hydrated microspheres.

The observation of coated MC aggregating in cell culture medium, which occurred only for LN on bare PS (Supplementary Fig. S1A; Supplementary Data are available online at www.liebertpub.com/scd), is not attributed to surface charge neutralization, given that PLL-coated MC retain a

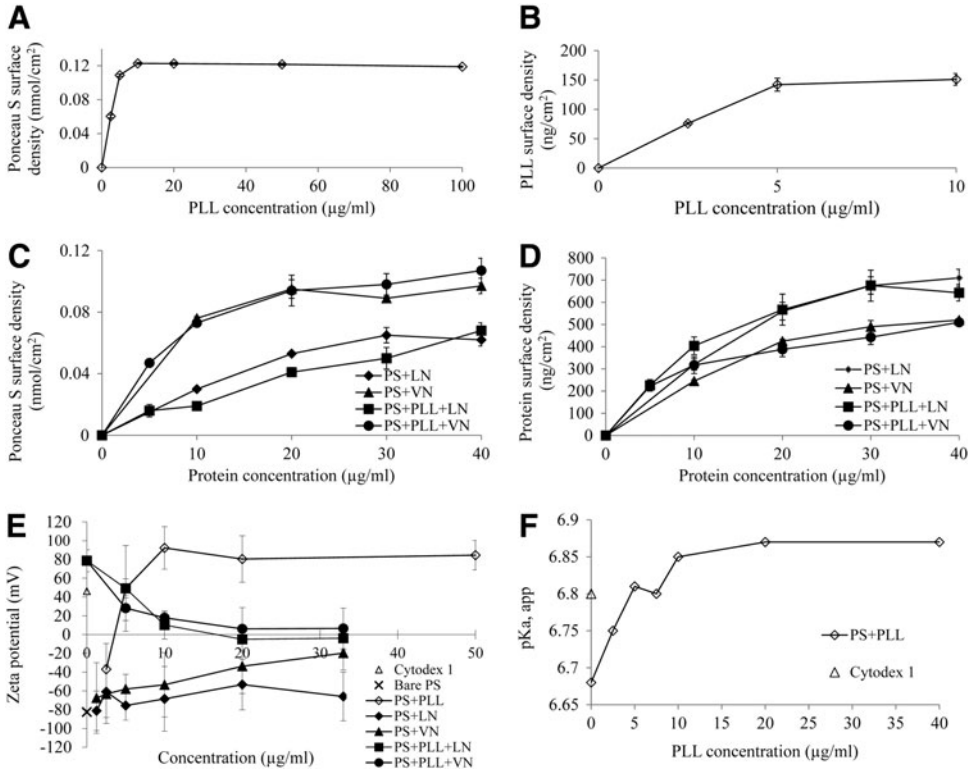

FIG. 1. Characterization of MC surface properties. PLL adsorbed to PS MC versus concentration of the depositing solution: **(A)** Ponceau S staining of the PLL coating, and **(B)** quantified PLL surface density. VN and LN adsorbed onto PS MC, bare and coated with PLL (PS + PLL), versus depositing solution concentration: **(C)** Ponceau S staining of the coated surface, and **(D)** surface density of VN and LN, respectively. **(E)** Zeta potential of bare and coated PS MC, and Cytodex 1. **(F)** pKa, app of PS MC coated with PLL, versus the depositing solution concentration, and of Cytodex 1. MC, microcarriers; LN, laminin; PLL, poly-L-lysine; PS, polystyrene; VN, vitronectin.

significant Zeta potential. This MC aggregation most likely arises from binding between the globular domains [51] situated at the extremities of LN arms, known to be tens of nanometers long [52,53]. A similar aggregation observed in PBS, without the divalent cations that induce LN molecules' aggregation [51,54,55], corroborates this hypothesis. The absence of a similar aggregation for MC coated with PLL + LN is putatively attributed to adsorbed LN molecules being more tightly bound, thus limiting their freedom to extend from the surface. This notion is substantiated by the efficient Zeta potential reduction for LN adsorbed on PLL (Fig. 1E), as compared with the residual surface charge density for LN on bare MC (Fig. 1D). VN molecules present a contrasting configuration, compact and roughly approximately by a cylinder of diameter 4.7 nm and length 11 nm [56]. This lower aspect ratio effectively compromises the ability of immobilized VN to bridge MC, despite the ability of these molecules to spontaneously aggregate in plasma [56] and on surfaces [34,57]. As described later, MC aggregation before hESC seeding has a significant impact on the MC's ability to form hESC/MC aggregates, which regulate the fold expansion of these cells.

ECM coatings

Initial cell attachment is critical for anchorage-dependent cell cultures, particularly for their implementation in stirred bioreactor systems [30]. To evaluate this seeding efficiency, an hESC (HES-3) single-cell suspension was seeded with a ratio of ~25 cells per MC in mTeSR1 medium. Attachment rates and the fraction of cells attached after 2 h, in static conditions and under agitation, are shown in Fig. 2. Positively charged Cytodex 1 served as a positive control, while bare MC provided a negative control [25].

Although efficient hESC attachment onto MC coated with ECM proteins was readily achieved in static conditions (Fig. 2A, C), there was a sharp decrease in attachment rates and the efficiency after 2 h under agitation (Fig. 2B, D). Cytodex 1 induces high cell efficiency attachment, both in static conditions and under agitation, implying that a cationic charge may enhance MC performance in cell seeding and thus prompting the introduction of a cationic PLL coating.

Combined PLL and ECM coatings

Attachment efficiency under agitation is recovered by introducing a cationic polyelectrolyte (PLL) coating, which adsorbs the adhesion-promoting ECM protein. Although MC coated solely with PLL generated a minor improvement in hESC attachment efficiency, this was considerably improved by adsorbed ECM protein. Seeding under agitation, thus, became viable, with PLL + VN exhibiting an adequate performance and PLL + LN inducing a higher cell attachment efficiency, approaching that of the Cytodex 1 benchmark (Fig. 2B).

In static culture, hESC and MC sink to the bottom of the reactor, where cell seeding occurs during prolonged contact. In contrast, hESC seeding under agitation relies on collisions with MC, with only a brief time of contact. Thus, the seeding enhancement generated by PLL indicates a charge attraction, which is putatively attributed to negatively charged sialic acid, presented at the surface of the cells [58]. A similar attachment observed for dead cells (glutaraldehyde-treated, data not shown) confirmed that initial adhesion can partially be attributed to passive binding. The Debye screening length of cell culture medium is estimated at less than 1 nm (c.f. 0.7 nm for 1× PBS [59]), which limits the range of electrostatic attractions to the close proximity of contact. Moreover, the low Zeta potential values of MC coated with PLL + VN or PLL + LN imply the absence of a surface electrical double layer. Notwithstanding these data, PLL significantly enhances hESC seeding efficiency, when

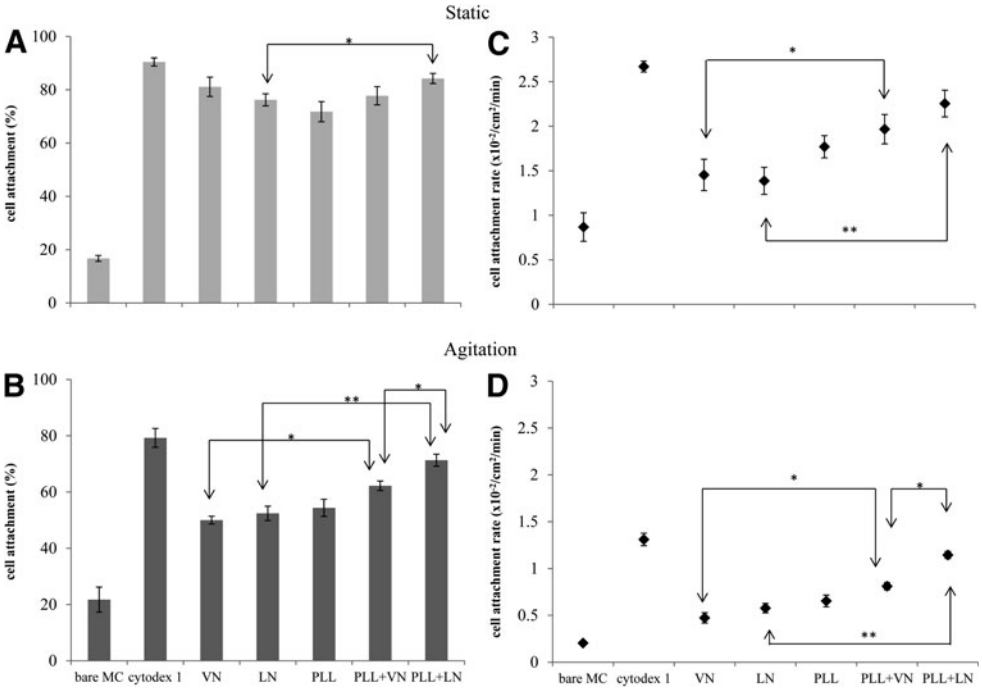

FIG. 2. HES-3 cell attachment efficiency, on coated PS MC, during the initial 2 h after seeding: **(A)** in static conditions and **(B)** under agitation. Cell attachment rates over the same time period: **(C)** in static conditions and **(D)** under agitation. * and ** indicate $P < 0.05$ and $P < 0.01$, respectively.

used in combination with an adsorbed coating of adhesion-promoting ECM protein.

Cell spreading, as inferred from the ratio of the cell's base length to its height (Fig. 3A), reveals a requirement for exogenous surface-immobilized ECM protein and corroborates a previous report of a minimum VN surface density to promote hESC adhesion and support their expansion [34]. Cells do not spread on PLL-coated MC, as indicated by their persistent quasi-spherical shape (L/H ≈ 1). In contrast, cells attached to ECM protein coatings spread within 2 h (Fig. 3B), with efficiency trends matching those for cell attachment under agitation (Fig. 2B). Interestingly, the indistinguishable spreading rates between static and agitated conditions indicate that hydrodynamic forces and collisions generated by agitation do not affect this process (Fig. 3B). The observed differences in cell spreading rates become redundant after 5 h, when HES-3 achieve L/H ≈ 4–5 on all MC coated with ECM protein (Fig. 3C).

The interaction of negatively charged heparan sulphate glycosaminoglycans in the hESC ECM with the underlying cationic charge enhances cell spreading on PLL + ECM protein coatings. Glycosaminoglycans synergize with syndecan proteoglycans and mediate ligand binding to integrins [60]. They are known to influence intra-cellular signaling [61], which impacts cell spreading and migration.

Static cultures do not distinguish between the performance of VN and LN in supporting hESC expansion [18], whereas cell seeding under agitation reveals enhanced hESC attachment and spreading [62] on LN, as compared with VN (Figs. 2B and 3B). Cell adhesion is mediated by endogenous integrins binding to ligands in ECM proteins coating the MC [63]. The αVβ5 integrin expressed in hESC binds to the single Arginine-Glycine-Aspartic acid (RGD) ligand presented by a VN molecule [64] with a dissociation constant (K_d) of 0.2 μM [65]. In contrast, hESC adhesion to LN is mediated by the α6β1 integrin. This can interact with two binding sites, one on the β1 chain and the other within the globular domains at the terminus of the α1 chain in LN [20]. This binding interaction is reported to be an order of magnitude stronger, with $K_d \approx 10$ nM [66], and is probably complemented by binding of the 67 kDa LN receptor, which has a high binding affinity ($K_d = 2$ nM [67]) and is ubiquitous in mammalian cells [68]. These elements lend substance to integrin-mediated hESC adhesion, accounting for the cell seeding and spreading performance of LN being enhanced over VN. As described later, these ECM proteins exhibit a similar performance differential in promoting the formation of hESC/MC aggregates, particularly when they are adsorbed onto a PLL coating.

Previous reports revealed a single-cell suspension to be problematic, primarily due to dissociation-induced cell apoptosis [69] resulting in poor cell adhesion. Although this drawback can be mitigated by culturing with the Rho-associated coiled kinase inhibitor [69,70] or using an LN E8 fragment [28] immobilized on the culture substrate, these solutions have limitations. The versatile enabling technology introduced in the present study enables hESC to propagate from a single-cell suspension, in agitated or stirred culture. The innovation relies on MC coated with cationic polyelectrolyte and adsorbed ECM protein, without requiring additional supplements.

Aggregate evolution determines hESC fold expansion

The initial attachment and spreading of hESC is followed by the establishment of a cytoskeleton, which plays a central role in cell mitosis and, thus, expansion [71]. Since hESC

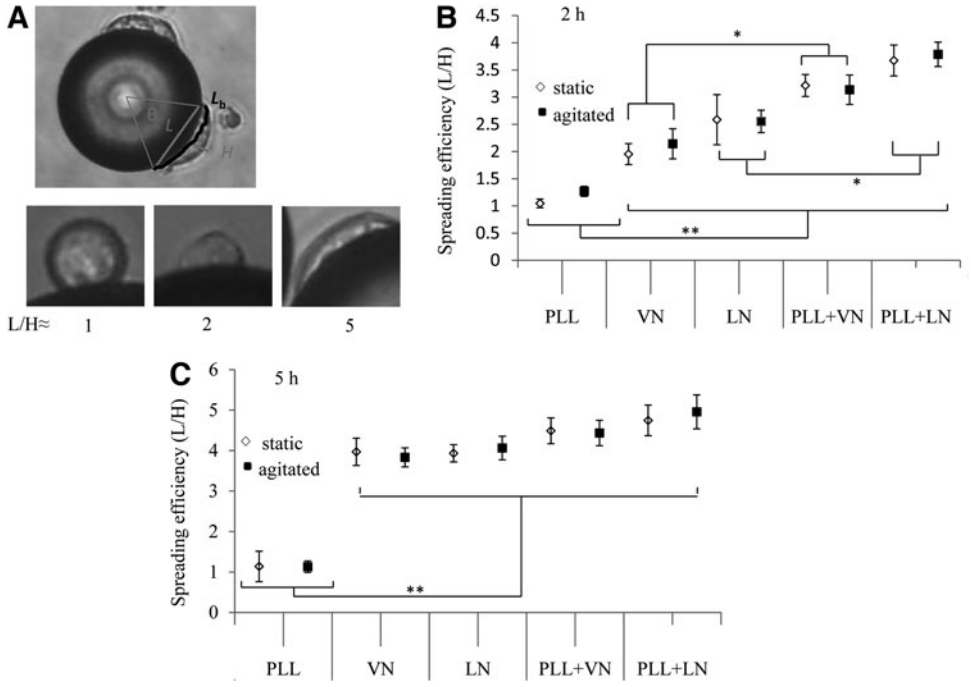

FIG. 3. HES-3 spreading on coated PS MC. **(A)** L, H definition and representative images of single hESC cells with increasing L/H values, corresponding to progressive stages of spreading. hESC spreading in static and agitated cultures after **(B)** 2 h and **(C)** 5 h of cell seeding; * and ** indicate $P < 0.05$ and $P < 0.01$, respectively. hESC, human embryonic stem cells; H, height; L, length.

grow within clusters on planar substrates [18,34], their 3D culture on MC relies on the formation of hESC/MC aggregates, which incorporate nearly all the free MC and can grow to large sizes in static conditions (Supplementary Fig. S2A and Ref. [18]). hESC culture in static conditions yielded a similar six- to eight-fold expansion, over 7 days, for all coated MC (Supplementary Fig. S2B). Nevertheless, hESC/MC aggregates resting at the bottom of the container are unsuited for volumetric scale up in 3D bioreactors, due to limitations in supplying nutrients and gases to the cells.

Agitation breaks up large hESC/MC aggregates into smaller, quasi-spherical clusters (Fig. 4 and Supplementary Fig. S1A, B), whose evolution determines hESC fold expansion at 7 days' culture. To elucidate how surface properties impact the evolution of aggregates, single hESC seeded onto coated MC were subjected to three culture regimes. These were designed to gradually increase the agitation stress: A 2-day static pause followed by 5 days' agitation (2 days static), a 1-day pause with 6 days' agitation (1 day static), and 7 days' continuous agitation (0 day static).

hESC expansion on MC coated solely with VN and LN

The initial formation of hESC/MC aggregates is a critical factor in determining cell viability and final expansion yields. Bare MC coated with ECM proteins exhibit poor performance in this regard, as seen by monitoring the evolution of hESC/MC aggregates. Under continuous agitation, MC coated with VN are unable to recruit free MC (Fig. 5), resulting in the absence of hESC/MC aggregates (Fig. 5 and Supplementary S1A) and low fold expansion (Fig. 4). The introduction of a static interval enables hESC/MC aggregates to form, which grow in size to more than 100 μm after a 1-day pause and 200 μm after a 2-day pause (Table 1). While the former increase hESC yield minimally, the latter generate significantly higher fold expansion at 7 days' culture (Fig. 4), even after a decrease in aggregate size with the resumption of agitation (Table 1). While aggregates evolve by recruiting free MC, their growth under agitation occurs via an increasing number density per unit volume and is associated with a modest increase in size (Fig. 5 and Table 1).

Seeded hESC adhere primarily to the exterior of LN-coated MC aggregates, which form before their exposure to the cells (Supplementary Fig. S1A). Over the course of 7 days' continuous agitation, the disintegration of these aggregates prevents the formation of hESC/MC aggregates and exposes the cells to collisions, both of which putatively lead to low cell yields. The introduction of a static pause, for 1 or 2 days, generates a significant increase in fold expansion at 7 days' culture. This interval appears to enable cells to grow within the MC aggregates, enabling the formation of a cell culture microenvironment and progressively increasing cell yields (Fig. 4).

As for VN-coated MC earlier, hESC/MC aggregates are reduced in size on resuming agitation. However, they do not recruit free MC and show little evolution, with no increase in their number density and only a modest increase in their

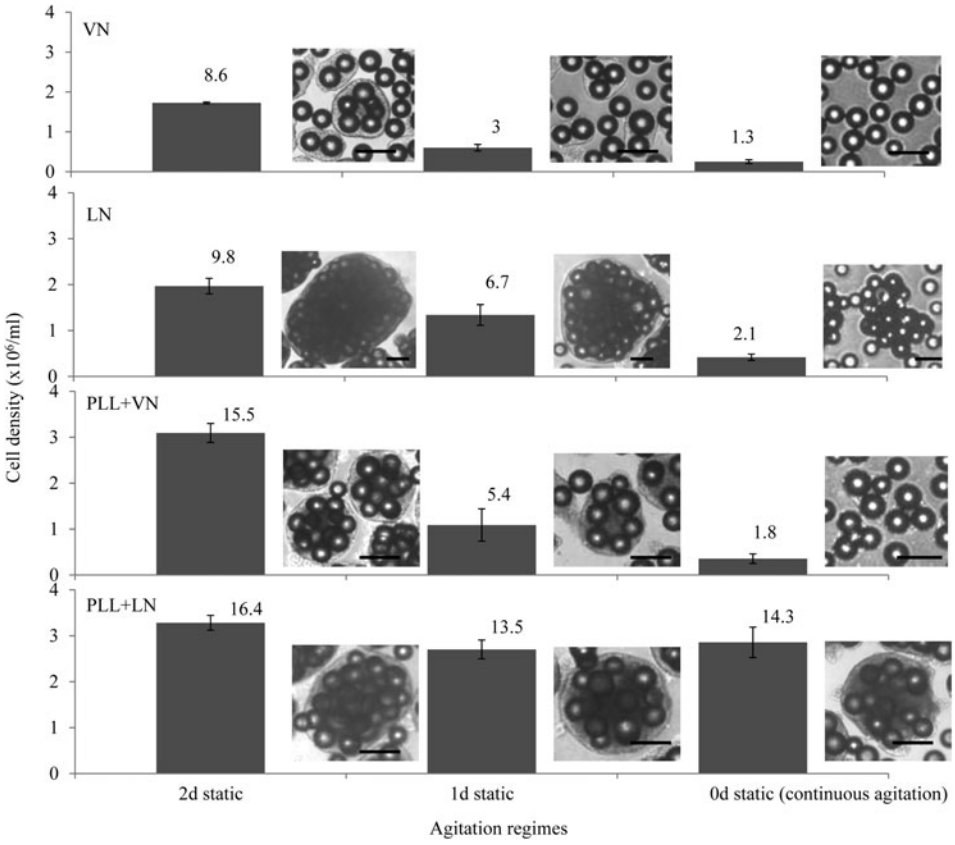

FIG. 4. HES-3 expanded on coated PS MC with different agitation regimes: 2 days' static + 5 days' agitation (2 days' static), 1 day static + 6 days' agitation (1 day static), and 7 days' continuous agitation (0 day static). Histogram bars indicate fold expansion, while images show representative hESC/MC aggregates at 7 days' culture. Scale bars are 200 μm.

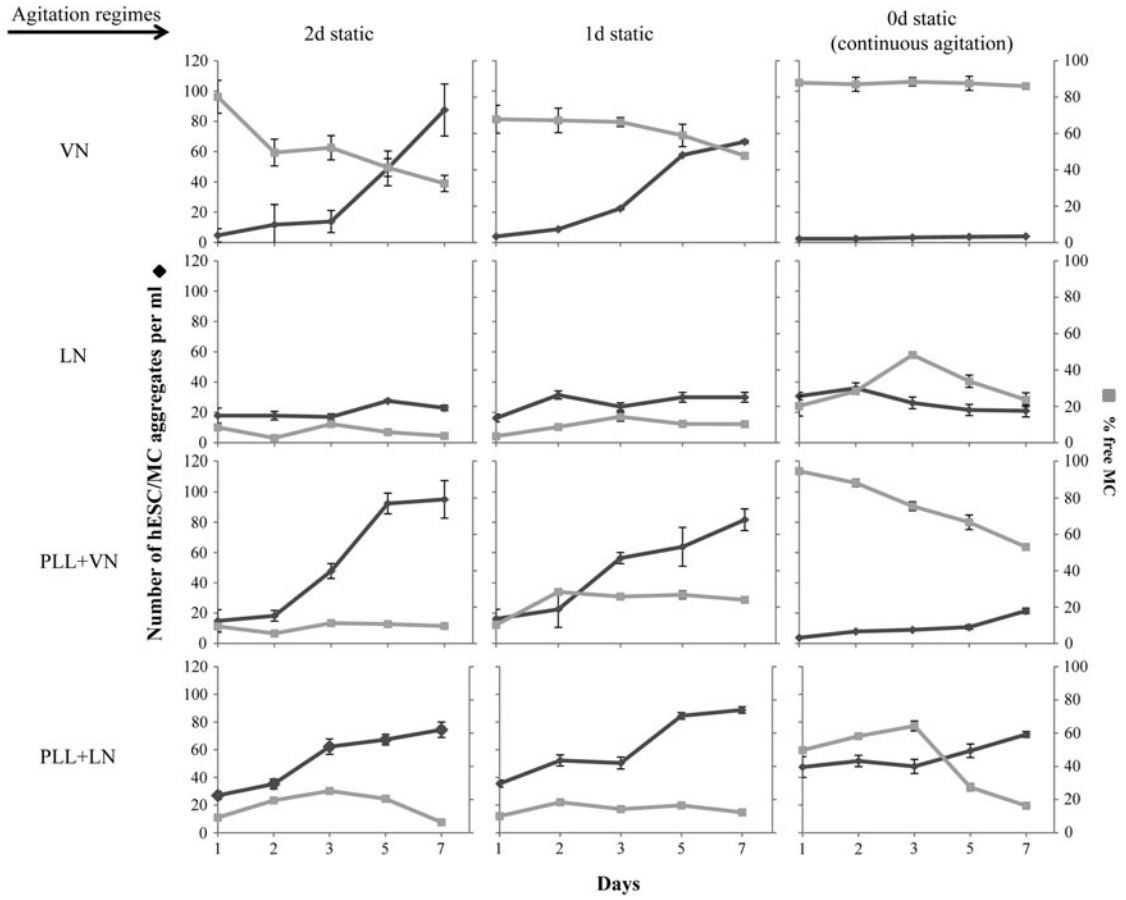

FIG. 5. Evolution of the hESC/MC aggregate number density and the percentage of free MC over 7 days' culture, for coated PS MC under each agitation regime. Lines joining the data points are guides for the eye.

TABLE 1. KINETICS SIZE OF HESC/MC AGGREGATES FORMATION, DURING HES-3 GROWTH ON COATED PS MC (VN, LN, PLL + VN, AND PLL + LN) IN THREE DIFFERENT AGITATION REGIMES

		hESC/MC aggregates size (μm)			
Agitation regimes	*Days*	*VN*	*LN*	*PLL + VN*	*PLL + LN*
2 days' static					
	1	120 ± 11	560 ± 20	360 ± 18	570 ± 13
	2	200 ± 18	710 ± 30	600 ± 20	620 ± 13
	3	160 ± 13	560 ± 14	430 ± 20	310 ± 10
	5	190 ± 11	580 ± 18	280 ± 13	330 ± 10
	7	230 ± 14	610 ± 14	290 ± 13	340 ± 10
1 day static					
	1	130 ± 10	610 ± 13	370 ± 19	600 ± 11
	2	130 ± 10	380 ± 10	190 ± 10	360 ± 10
	3	160 ± 3	470 ± 11	200 ± 17	320 ± 10
	5	190 ± 3	510 ± 10	210 ± 3	330 ± 10
	7	200 ± 11	530 ± 11	230 ± 10	330 ± 10
0 day static (continuous agitation)					
	1	120 ± 10	470 ± 15	140 ± 17	280 ± 13
	2	120 ± 13	470 ± 18	130 ± 10	280 ± 10
	3	130 ± 11	430 ± 19	130 ± 10	310 ± 10
	5	150 ± 13	370 ± 17	160 ± 10	320 ± 10
	7	150 ± 30	370 ± 14	170 ± 10	320 ± 11

hESC, human embryonic stem cells; LN, laminin; PLL, poly-L-lysine; PS, polystyrene; VN, vitronectin.

size. Despite large hESC/MC aggregates ($\approx$ 400–600 μm) remaining throughout the culture period, fold expansion remains significantly lower than that generated by MC with a cationic polyelectrolyte and ECM protein coating (Fig. 4), illustrating that MC aggregation *per se* is not sufficient to generate optimal hESC growth in a stirred culture environment.

MC coated with PLL + VN

The coating combination of PLL and ECM protein induces a different formation and a progressive evolution of the hESC/MC aggregates. MC coated with PLL + VN are unable to form sizable hESC/MC aggregates (120–150 μm) under continuous agitation, despite a modest recruitment of free MC. This results in low expansion yields, which are remedied by introducing a static pause, enabling larger hESC/MC aggregates to form (Table 1). Cell yields increase significantly after a 1-day static pause, and these become remarkably high after a 2-day static pause (Fig. 4). The hESC/MC aggregates evolve during the static pause, increasing their size to 360 μm after 1 day and 600 μm after 2 days (Table 1). Images of hESC/MC show the progressive incorporation of free MC during the 1- or 2-day static pause (Supplementary Fig. S1B), with a few free MC incorporated after the resumption of agitation (Fig. 5). Despite agitation reducing the average aggregate dimensions, these retain sizes of 200 and $>$300 μm, after a 1- or 2-day static interval, respectively. This difference in initial aggregate size critically influences cell growth, generating three-fold higher yields, comparable to those arising from MC coated with PLL + LN (as described next). Moreover, cell expansion occurs by increasing the aggregate number density, while maintaining their average size almost unchanged.

MC coated with PLL + LN

A coating of PLL + LN induces the formation of hESC/MC aggregates and supports their progressive evolution. As for MC coated with PLL + VN, cell expansion results in a steady increase in the number density of hESC/MC aggregates, with only a modest increase in average size. A salient feature of MC coated with PLL + LN is that they induce the formation of hESC/MC aggregates of a sufficient size ($\approx$ 300 μm) under continuous agitation. The introduction of a 1- or a 2-day pause in the agitation increases the size of hESC/MC aggregates to $\approx$600 μm, and this is, subsequently, reduced to $\approx$300 μm on resuming agitation. Thus, regardless of the agitation regime, MC coated with PLL + LN generate remarkably high fold expansion ($\approx$ 13–16, Fig. 4), equivalent to the cell yields offered by MC coated with PLL + VN after a 2-day static pause (Table 1 and Supplementary Fig. S1B).

Correlation between hESC/MC aggregate size and cell expansion

Figure 6 shows a correlation, drawn between fold expansion at 7 days' culture and the hESC/MC aggregate size or number density, respectively. The latter were measured at 1 day after the onset of agitation, during their initial stage of evolution, and before the onset of peak cell growth. The data are clustered into two domains. The high fold-expansion domain, defined as 13–15 times the number of seeded cells, is generated by MC coated with PLL + LN under all three agitation regimes and MC coated with PLL + VN ensuing after a 2-day static pause. These hESC/MC aggregates have dimensions of at least 300 μm and number densities exceeding $\approx$50/mL. Within the lower fold-expansion domain, a modest correlation between hESC/MC aggregate dimensions and final cell yields underpins their formation being essential for cell growth. Nevertheless, aggregate dimensions below 200 μm and number densities <40/mL do not give rise to high hESC yields at 7 days' culture. LN-coated MC are not shown, due to their forming large aggregates before cell contact and the lack of a progressive evolution of the hESC/MC aggregates, which give rise to low cell yields.

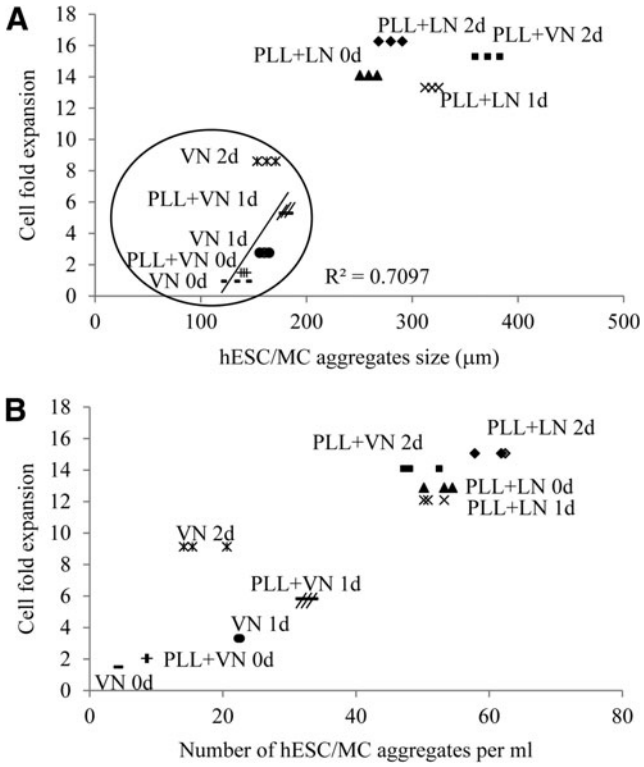

FIG. 6. Scatter plot of **(A)** hESC/MC aggregate size and **(B)** number density of aggregates, versus fold expansion of cells after 7 days' culture. Data are for HES-3 cultured on coated PS MC, except LN-coated PS, for each of the three agitation regimes. Both the sizes and numbers were measured at the onset of agitation on day 1; while the cell expansion fold was measured at day 7. A low expansion domain is encircled, and the straight line correlates with data points within it.

Formation and evolution of hESC/MC aggregates

It has been suggested that stem cells reside in a dynamic, specialized microenvironment, denoted as the stem cell niche, which plays an important role in cell survival and maintains a balance between self-renewal and differentiation [72]. Key components that sustain the niche include growth factors, cell–cell interactions, and cell–matrix (ECM) adhesions [73]. Peerani et al. [74] also illustrated

that one way to regulate niche interactions is by controlling the size of hESC colonies, which will limit the secretion of growth factors within the microenvironment. They also demonstrated that endogenous signaling and pluripotent gene expression change with colony size. The minimal size for the maintenance and expansion of hESC is about 200–400 μm in diameter, with larger colonies with local high cell density microenvironments promoting the maintenance of the undifferentiated phenotype in hESC. Diameters inferior to 200 μm affect the proliferation of hESC and the trajectory of its differentiation. This is concomitant to our results that hESC/MC aggregates with dimensions of at least 300 μm result in high hESC yields.

An earlier murine stem cell study by the same group describes self-regulating niche dimensions, based on the cells' response to a radially distributed autocrine self-renewal signal [75]. It is likely that analogous cell signaling with a radial distribution may play a role in regulating the size of hESC/MC aggregates, which attain average dimensions of ≈300–330 μm under agitation. This size regulation is reflected in the reduction in size of hESC/MC aggregates, formed by MC coated with PLL + LN during the static pause, from ≈600 to ≈300 μm with the onset of agitation. It also appears to be responsible for the cell expansion process being associated with an increase in the number density of aggregates, while their linear dimensions show only modest growth. The latter is observed for MC coated with PLL + VN after a static pause and for MC coated with PLL + LN under all agitation regimes (Fig. 5 and Table 1). However, the ≈ 200 μm hESC/MC aggregates generated by MC coated with PLL + VN after a 1-day static pause are unable to increase their average size under agitation. They remain below the critical size of ≈300 μm, with a corresponding three-fold reduction in hESC yields at 7 days' culture, as described earlier.

Time-lapse evolution of aggregate growth

A perspective on the evolution of hESC/MC aggregates is offered by time-lapsed images of a single free MC being incorporated into an aggregate (Fig. 7). Although a sole ECM protein coating promotes the attachment of a free MC, this remains on the exterior of the aggregate, without being engulfed by the cells, even after 24 h. ECM proteins coated onto PLL generate a fundamentally different behavior: The free MC is engulfed by the hESC/MC aggregate through a phenomenon that is putatively regulated by hESC migration. Following the same trend as for hESC spreading (Fig. 3), the incorporation of a free MC occurs at different time scales: MC coated with PLL + VN are engulfed by hESC after 16.5 ± 1.6 h, while those coated with PLL + LN require only 9.4 ± 0.8 h (Fig. 7). Given the static nature of this experiment, these data highlight clear differences between the performance of a sole ECM protein coating and the same with an underlying cationic polyelectrolyte. Moreover, these data corroborate the evolution of hESC/MC aggregates over the static interval: A coating of PLL + VN forms 360 μm aggregates over 1 day, while aggregates formed by PLL + LN attain 600 μm over the same time period (Table 1).

Cell viability and pluripotency

Pluripotent marker expression was uniformly high for hESC expanded on coated MC under all agitation regimes, with the exception of cells cultured on sole ECM protein coatings under continuous agitation. The latter exhibit a pluripotency loss that is associated with very low cell yields (less than two-fold) (Supplementary Fig. S3). Pluripotency was maintained following three passages under agitation, and cell viability from all cultures was above 90%. This

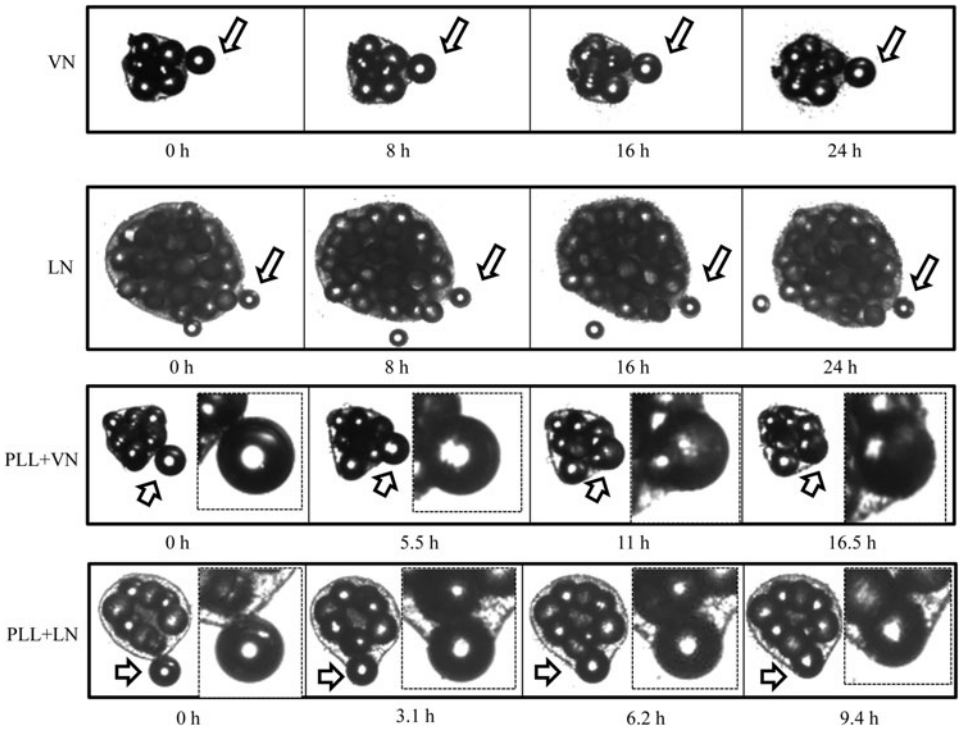

FIG. 7. Time-lapse images of a free MC being incorporated into hESC/MC aggregates, formed by HES-3 and coated PS MC. For PLL + VN and PLL + LN, the insets magnify the free MC incorporation process. *Arrows* indicate cells spreading on an individual MC.

establishes that, irrespective of fold expansion, cells expanded in cultures that form and evolve hESC/MC aggregates remain viable and pluripotent.

Although the formation of aggregates is a stochastic process, coated MC give rise to a highly reproducible formation of hESC/MC aggregates, as substantiated by three separate trials with indistinguishable aggregate evolution and final fold expansion at 7 days' culture (Supplementary Fig. S4). One of the most interesting findings is the universality of the impact that coated MC have on hPSC (hESC and hiPSC) culture development. This was demonstrated with another hESC line (HES-7) and an hiPSC cell line (IMR90), both of which are cultured on MC coated with PLL + VN and PLL + LN, respectively, using the same three agitation regimes. The identical trends in hESC/MC aggregate development and fold expansion at 7 days' culture (Supplementary Figs. S5A, B) substantiate the robustness of this cell expansion environment and its associated process. Given that all three cell lines putatively express the same endogenous integrins and adhesion-promoting receptors [67], their bioresponse to the MC surface properties regulates the evolution of hESC/MC aggregates, giving rise to highly reproducible and robust cell yields under these agitation regimes.

Scaling up PLL + VN and PLL + LN cultures in spinner flasks

An essential proof of concept is the scale up of this hESC culture MC matrix in stirred spinner flasks. MC coated with PLL + VN and PLL + LN were used as matrices for the culture hESC in the stirred environment of spinner flasks. The cell culture was seeded with hESC/MC aggregates, which were formed under agitation as described earlier. These aggregates were broken down to dimensions of 250 μm, in order to generate more nuclei for cell growth. A 1-day static interval was then introduced for the PLL + LN coating and a similar 2-day interval was used for PLL + VN, to ensure their stabilization [14,25] before applying continuous stirring for a total of 9 days' culture.

The stirred culture exhibited an initial lag period of 3 and 4 days, for the PLL + VN and PLL + LN coatings, respectively, during which about three quarters of the free MC were integrated into the existing hESC/MC aggregates (Fig. 8B, D). This was followed by a sustained period of high-rate cell expansion (Fig. 8A, C). This phase exhibited a steady increase in the number density of hESC/MC aggregates, with only a modest increase in their size, in a manner similar to that described earlier for cultures under agitation. These cultures resulted in a similarly high fold expansion, with expanded hESC viability higher than 90%. An analysis of pluripotent marker expression revealed that more than 95% of the cell population was positive for Tra-1-60, Oct-4, and mAb84 (Fig. 9A) and their ability to differentiate was evaluated with EB, which stained positive for representative markers of the three primary germ layers: AFP for endoderm, SMA for mesoderm, and β-III-tubulin for ectoderm (Fig. 9B). This was corroborated by an increased expression of six lineage-specific genes and a decreased Oct-4 expression, as measured by real-time PCR (Fig. 9C).

A further assessment of the cells' differentiation ability was assessed by inducing their differentiation into cardiomyocytes with the Wnt inhibitors' protocol [48,76]. Approximately 41% of the final cell population stained positive for cTnT, and about 33% was positive for MF20 (Supplementary Fig. S6). Contractile regions were observed in the plated cells at days 10–12 (Supplementary Movie S1). These results demonstrate that hESC propagated on MC coated with a cationic polyelectrolytes and an appropriate ECM protein remain pluripotent and retain their ability to

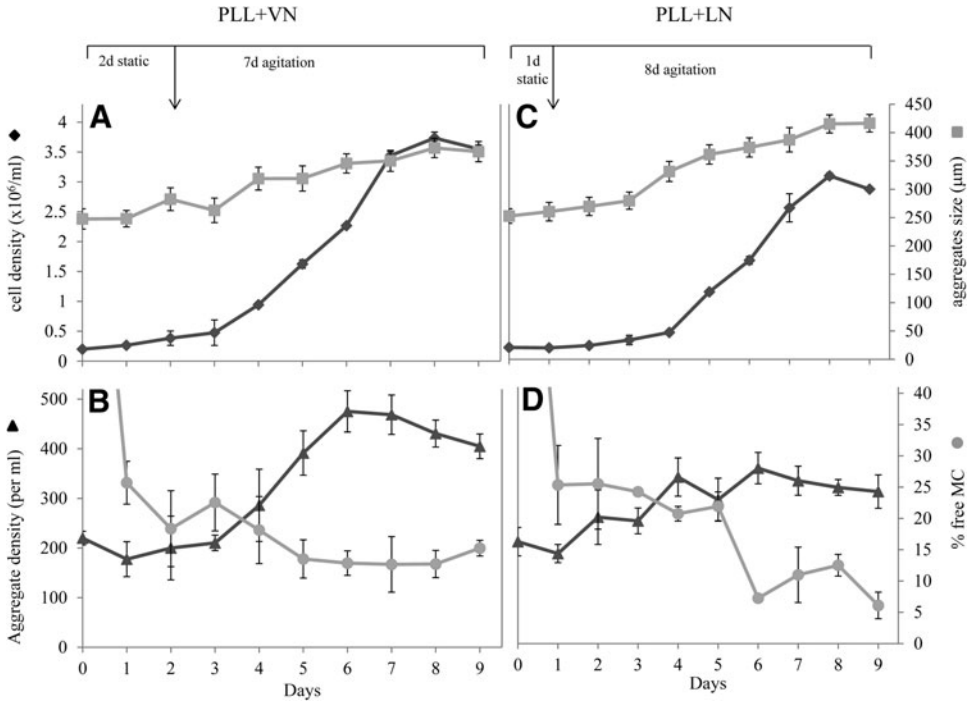

FIG. 8. Evolution of HES-3 expansion in spinner flasks. Static pauses of 1- and 2 days were introduced for PS MC coated with PLL + LN and PLL + VN, respectively, to stabilize the hESC/MC aggregates before agitation. Parts **(A)** and **(C)** depict hESC cell density and the size of hESC/MC aggregates over 9 days' culture, while parts **(B)** and **(D)** show the number density of hESC/MC aggregates and the percentage of free MC, for PS MC coated with PLL + VN and PLL + LN, respectively.

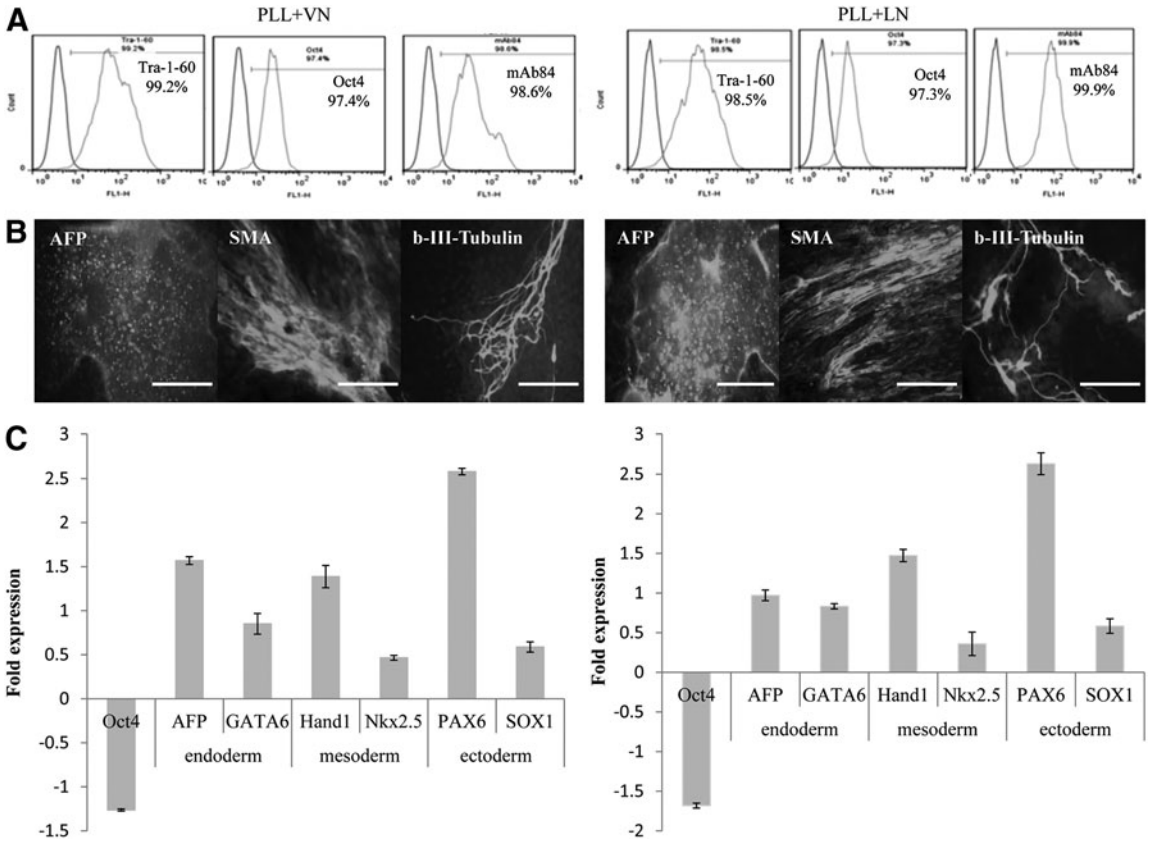

FIG. 9. Characterization of HES-3 cells expanded in spinner flasks on PS MC with PLL + VN and PLL + LN coatings, respectively. **(A)** FACS of pluripotent markers. For differentiated HES-3: **(B)** images of immunochemical staining for markers associated with the three embryonic germ layers, AFP (endoderm), SMA (mesoderm), and β-III tubulin (ectoderm). Scale bars are 200 μm. **(C)** quantitative RT-PCR data for a pluripotent marker gene and genes associated with the formation of the three primary germ layers. FACS, fluorescence-activated cell sorting; RT-PCR, reverse transcription-polymerase chain reaction.

differentiate into the three primary germ layers, as well as the specific cardiomyocyte lineage.

In summary, defined and characterized PS MC coated with ECM proteins and positive charge were implemented in a systematic study to investigate the critical parameters that influence hESC expansion in a serum-free medium, under agitation or stirring. The introduction of a cationic polyelectrolyte layer, underlying a coating of adhesion-promoting ECM protein, VN, or LN, fulfilled the essential prerequisite of efficient initial cell attachment and spreading. Integrin-mediated binding and a specific receptor putatively promote higher attachment and spreading efficiencies for LN, as compared with VN.

The subsequent formation of hESC/MC aggregates enables cell viability and results in high cell yields. Sole ECM proteins form sub-optimal aggregates and these same proteins coated onto PLL form aggregates that evolve progressively under agitation. A critical aggregate size of $\approx 300\,\mu m$ and a number density of ≈ 50/mL, measured 1 day after the onset of agitation, are required for high fold expansion at 7 days' culture. Smaller aggregates ($\approx 200\,\mu m$) result in significantly lower cell yields. Cell expansion is associated with increasing number density of hESC/MC aggregates, at a quasi-constant size that does not exceed 300–340 μm. This implies a self-regulating microenvironment, within which hESC propagate and retain their pluripotency [74]. MC coated with PLL + VN necessitate a 2-day static pause to achieve high (≈ 15) fold expansion. In contrast, MC coated with PLL + LN support the formation of aggregates under continuous agitation, thus enabling a scalable expansion process that is compatible with bioreactors.

The highly reproducible evolution of hESC/MC aggregates and their corresponding cell yields was confirmed over several trials. This robustness was further substantiated by the bioresponse of second hESC and hiPSC lines, both of which evolved hESC/MC aggregates following quasi-identical trends as HES-3 cells. Finally, experiments in stirrer flasks validated the potential of this hESC expansion environment for scalable bioreactors. Pluripotent marker expression remained high, and cells retained their ability to differentiate, including forming cardiomyocytes. This technology is an important step in providing a system that generates large quantities of hESC in a defined environment, for future cell therapies.

Acknowledgment

The authors thank the Joint Council Office of the Agency of Science and Technology (A*STAR) for funding this project.

Author Disclosure Statement

No competing financial interests exist.

References

1. Kobayashi S, T Takebe, M Inui, S Iwai, H Kan, YW Zheng, J Maegawa and H Taniguchi. (2011). Reconstruction of human elastic cartilage by a $CD44^+$ $CD90^+$ stem cell in the ear perichondrium. Proc Natl Acad Sci U S A 108: 14479–14484.
2. Kriks S, JW Shim, J Piao, YM Ganat, DR Wakeman, Z Xie, L Carrillo-Reid, G Auyeung, C Antonacci, et al. (2011). Dopamine neurons derived from human ES cells efficiently engraft in animal models of Parkinson's disease. Nature 480:547–551.
3. Lu SJ, F Li, H Yin, Q Feng, EA Kimbrel, E Hahm, JN Thon, W Wang, JE Italiano, J Cho and R Lanza. (2011). Platelets generated from human embryonic stem cells are functional in vitro and in the microcirculation of living mice. Cell Res 21:530–545.
4. Schwartz SD, JP Hubschman, G Heilwell, V Franco-Cardenas, CK Pan, RM Ostrick, E Mickunas, R Gay, I Klimanskaya and R Lanza. (2012). Embryonic stem cell trials for macular degeneration: a preliminary report. Lancet 379:713–720.
5. Segers VF and RT Lee. (2008). Stem-cell therapy for cardiac disease. Nature 451:937–942.
6. Chun YS, K Byun and B Lee. (2011). Induced pluripotent stem cells and personalized medicine: current progress and future perspectives. Anat Cell Biol 44:245–255.
7. Bardy J, AK Chen, YM Lim, S Wu, S Wei, H Weiping, K Chan, S Reuveny and SK Oh. (2013). Microcarrier suspension cultures for high-density expansion and differentiation of human pluripotent stem cells to neural progenitor cells. Tissue Eng Part C Methods 19:166–180.
8. Lecina M, S Ting, A Choo, S Reuveny and S Oh. (2010). Scalable platform for human embryonic stem cell differentiation to cardiomyocytes in suspended microcarrier cultures. Tissue Eng Part C Methods 16:1609–1619.
9. Leung HW, A Chen, AB Choo, S Reuveny and SK Oh. (2011). Agitation can induce differentiation of human pluripotent stem cells in microcarrier cultures. Tissue Eng Part C Methods 17:165–172.
10. Lock LT and ES Tzanakakis. (2009). Expansion and differentiation of human embryonic stem cells to endoderm progeny in a microcarrier stirred-suspension culture. Tissue Eng Part A 15:2051–2063.
11. Chen AK, S Reuveny and SK Oh. (2013). Application of human mesenchymal and pluripotent stem cell microcarrier cultures in cellular therapy: achievements and future direction. Biotechnol Adv 31:1032–1046.
12. Kehoe DE, D Jing, LT Lock and ES Tzanakakis. (2010). Scalable stirred-suspension bioreactor culture of human pluripotent stem cells. Tissue Eng Part A 16:405–421.
13. Nie Y, V Bergendahl, DJ Hei, JM Jones and SP Palecek. (2009). Scalable culture and cryopreservation of human embryonic stem cells on microcarriers. Biotechnol Prog 25: 20–31.
14. Oh SK, AK Chen, Y Mok, X Chen, UM Lim, A Chin, AB Choo and S Reuveny. (2009). Long-term microcarrier suspension cultures of human embryonic stem cells. Stem Cell Res 2:219–230.
15. Serra M, C Brito, MF Sousa, J Jensen, R Tostoes, J Clemente, R Strehl, J Hyllner, MJ Carrondo and PM Alves. (2010). Improving expansion of pluripotent human embryonic stem cells in perfused bioreactors through oxygen control. J Biotechnol 148:208–215.
16. Marinho PA, DT Vareschini, IC Gomes, S Paulsen Bda, DR Furtado, R Castilho Ldos and SK Rehen. (2013). Xeno-free production of human embryonic stem cells in stirred microcarrier systems using a novel animal/human-component-free medium. Tissue Eng Part C Methods 19:146–155.
17. Phillips BW, R Horne, TS Lay, WL Rust, TT Teck and JM Crook. (2008). Attachment and growth of human embryonic stem cells on microcarriers. J Biotechnol 138:24–32.
18. Heng BC, J Li, AK Chen, S Reuveny, SM Cool, WR Birch and SK Oh. (2012). Translating human embryonic stem cells from 2-dimensional to 3-dimensional cultures in a defined medium on laminin- and vitronectin-coated surfaces. Stem Cells Dev 21:1701–1715.
19. Newman KD and MW McBurney. (2004). Poly(D,L lactic-co-glycolic acid) microspheres as biodegradable microcarriers for pluripotent stem cells. Biomaterials 25: 5763–5771.
20. Domogatskaya A, S Rodin and K Tryggvason. (2012). Functional diversity of laminins. Annu Rev Cell Dev Biol 28:523–553.
21. Timpl R, H Rohde, PG Robey, SI Rennard, JM Foidart and GR Martin. (1979). Laminin—a glycoprotein from basement membranes. J Biol Chem 254:9933–9937.
22. Aumailley M, L Bruckner-Tuderman, WG Carter, R Deutzmann, D Edgar, P Ekblom, J Engel, E Engvall, E Hohenester, et al. (2005). A simplified laminin nomenclature. Matrix Biol 24:326–332.
23. Colognato H and PD Yurchenco. (2000). Form and function: the laminin family of heterotrimers. Dev Dyn 218: 213–234.
24. Miyazaki T, S Futaki, K Hasegawa, M Kawasaki, N Sanzen, M Hayashi, E Kawase, K Sekiguchi, N Nakatsuji and H Suemori. (2008). Recombinant human laminin isoforms can support the undifferentiated growth of human embryonic stem cells. Biochem Biophy Res Co 375:27–32.
25. Chen AK, X Chen, AB Choo, S Reuveny and SK Oh. (2011). Critical microcarrier properties affecting the expansion of undifferentiated human embryonic stem cells. Stem Cell Res 7:97–111.
26. Domogatskaya A, S Rodin, A Boutaud and K Tryggvason. (2008). Laminin-511 but not -332, -111, or -411 enables mouse embryonic stem cell self-renewal in vitro. Stem Cells 26:2800–2809.
27. Rodin S, A Domogatskaya, S Strom, EM Hansson, KR Chien, J Inzunza, O Hovatta and K Tryggvason. (2010). Long-term self-renewal of human pluripotent stem cells on human recombinant laminin-511. Nat Biotechnol 28:611–615.
28. Miyazaki T, S Futaki, H Suemori, Y Taniguchi, M Yamada, M Kawasaki, M Hayashi, H Kumagai, N Nakatsuji, K Sekiguchi and E Kawase. (2012). Laminin E8 fragments support efficient adhesion and expansion of dissociated human pluripotent stem cells. Nat Commun 3:1236.
29. Schvartz I, D Seger and S Shaltiel. (1999). Vitronectin. Int J Biochem Cell Biol 31:539–544.
30. Bueno EM, G Laevsky and GA Barabino. (2007). Enhancing cell seeding of scaffolds in tissue engineering through manipulation of hydrodynamic parameters. J Biotechnol 129:516–531.
31. Rowland TJ, LM Miller, AJ Blaschke, EL Doss, AJ Bonham, ST Hikita, LV Johnson and DO Clegg. (2010). Roles

of integrins in human induced pluripotent stem cell growth on Matrigel and vitronectin. Stem Cells Dev 19:1231–1240.
32. Braam SR, L Zeinstra, S Litjens, D Ward-van Oostwaard, S van den Brink, L van Laake, F Lebrin, P Kats, R Hochstenbach, et al. (2008). Recombinant vitronectin is a functionally defined substrate that supports human embryonic stem cell self-renewal via alphavbeta5 integrin. Stem Cells 26:2257–2265.
33. Li J, J Bardy, LY Yap, A Chen, V Nurcombe, SM Cool, SK Oh and WR Birch. (2010). Impact of vitronectin concentration and surface properties on the stable propagation of human embryonic stem cells. Biointerphases 5:FA132–FA142.
34. Yap LY, J Li, IY Phang, LT Ong, JZ Ow, JC Goh, V Nurcombe, J Hobley, AB Choo, et al. (2011). Defining a threshold surface density of vitronectin for the stable expansion of human embryonic stem cells. Tissue Eng Part C Methods 17:193–207.
35. Abbasalizadeh S, MR Larijani, A Samadian and H Baharvand. (2012). Bioprocess development for mass production of size-controlled human pluripotent stem cell aggregates in stirred suspension bioreactor. Tissue Eng Part C Methods 18:831–851.
36. Serra M, C Brito, C Correia and PM Alves. (2012). Process engineering of human pluripotent stem cells for clinical application. Trends Biotechnol 30:350–359.
37. Chisti Y. (2001). Hydrodynamic damage to animal cells. Crit Rev Biotechnol 21:67–110.
38. Hua J, LE Erickson, TY Yiin and LA Glasgow. (1993). A review of the effects of shear and interfacial phenomena on cell viability. Crit Rev Biotechnol 13:305–328.
39. Al-Rubeai M, RP Singh, MH Goldman and AN Emery. (1995). Death mechanisms of animal cells in conditions of intensive agitation. Biotechnol Bioeng 45:463–472.
40. Kretzmer G. (2000). Influence of stress on adherent cells. Adv Biochem Eng Biotechnol 67:123–137.
41. Kinney MA, CY Sargent and TC McDevitt. (2011). The multiparametric effects of hydrodynamic environments on stem cell culture. Tissue Eng Part B Rev 17:249–262.
42. Yu J, MA Vodyanik, K Smuga-Otto, J Antosiewicz-Bourget, JL Frane, S Tian, J Nie, GA Jonsdottir, V Ruotti, et al. (2007). Induced pluripotent stem cell lines derived from human somatic cells. Science 318:1917–1920.
43. Chin AC, J Padmanabhan, SK Oh and AB Choo. (2010). Defined and serum-free media support undifferentiated human embryonic stem cell growth. Stem Cells Dev 19: 753–761.
44. Bradford MM. (1976). A rapid and sensitive method for the quantitation of microgram quantities of protein utilizing the principle of protein-dye binding. Anal Biochem 72:248–254.
45. Ng YC, JM Berry and M Butler. (1996). Optimization of physical parameters for cell attachment and growth on macroporous microcarriers. Biotechnol Bioeng 50:627–635.
46. Choo AB, HL Tan, SN Ang, WJ Fong, A Chin, J Lo, L Zheng, H Hentze, RJ Philp, SK Oh and M Yap. (2008). Selection against undifferentiated human embryonic stem cells by a cytotoxic antibody recognizing podocalyxin-like protein-1. Stem Cells 26:1454–1463.
47. Maecker HT and J Trotter. (2006). Flow cytometry controls, instrument setup, and the determination of positivity. Cytometry A 69:1037–1042.
48. Lian X, C Hsiao, G Wilson, K Zhu, LB Hazeltine, SM Azarin, KK Raval, J Zhang, TJ Kamp and SP Palecek. (2012). Robust cardiomyocyte differentiation from human pluripotent stem cells via temporal modulation of canonical Wnt signaling. Proc Natl Acad Sci U S A 109:E1848–E1857.
49. Wang C, Y Gong, Y Lin, J Shen and DA Wang. (2008). A novel gellan gel-based microcarrier for anchorage-dependent cell delivery. Acta Biomater 4:1226–1234.
50. Stathopoulos NA and JD Hellums. (1985). Shear stress effects on human embryonic kidney cells in Vitro. Biotechnol Bioeng 27:1021–1026.
51. Yurchenco PD, EC Tsilibary, AS Charonis and H Furthmayr. (1985). Laminin polymerization in vitro. Evidence for a two-step assembly with domain specificity. J Biol Chem 260:7636–7644.
52. Nomizu M, A Utani, K Beck, A Otaka, PP Roller and Y Yamada. (1996). Mechanism of laminin chain assembly into a triple-stranded coiled-coil structure. Biochemistry 35:2885–2893.
53. Sasaki T, R Fassler and E Hohenester. (2004). Laminin: the crux of basement membrane assembly. J Cell Biol 164: 959–963.
54. Onuma K and N Kanzaki. (2005). Aggregation dynamics of laminin-1 in a physiological solution: A time-resolved static light scattering study. Journal of Crystal Growth 284: 530–537.
55. Onuma K and N Kanzaki. (2003). Size Distribution and Intermolecular Interaction of Laminin-1 in Physiological Solutions. J Phy Chem 107:11799–11804.
56. Izumi M, KM Yamada and M Hayashi. (1989). Vitronectin exists in two structurally and functionally distinct forms in human plasma. Biochim Biophys Acta 990:101–108.
57. Zhang H, K Bremmell, S Kumar and RS Smart. (2004). Vitronectin adsorption on surfaces visualized by tapping mode atomic force microscopy. J Biomed Mater Res A 68:479–488.
58. Janas T. (2011). Membrane oligo- and polysialic acids. Biochim Biophys Acta 1808:2923–2932.
59. Stern E, R Wagner, FJ Sigworth, R Breaker, TM Fahmy and MA Reed. (2007). Importance of the Debye screening length on nanowire field effect transistor sensors. Nano Lett 7:3405–3409.
60. Morgan MR, MJ Humphries and MD Bass. (2007). Synergistic control of cell adhesion by integrins and syndecans. Nat Rev Mol Cell Bio 8:957–969.
61. Lambaerts K, SA Wilcox-Adelman and P Zimmermann. (2009). The signaling mechanisms of syndecan heparan sulfate proteoglycans. Curr Opin Cell Biol 21:662–669.
62. Grinnell F. (1978). Cellular adhesiveness and extracellular substrata. Int Rev Cytol 53:65–144.
63. Plow EF, TA Haas, L Zhang, J Loftus and JW Smith. (2000). Ligand binding to integrins. J Biol Chem 275: 21785–21788.
64. Lynn GW, WT Heller, A Mayasundari, KH Minor and CB Peterson. (2005). A model for the three-dimensional structure of human plasma vitronectin from small-angle scattering measurements. Biochemistry 44:565–574.
65. Preissner KT, E Anders, J Grulich-Henn and G Muller-Berghaus. (1988). Attachment of cultured human endothelial cells is promoted by specific association with S protein (vitronectin) as well as with the ternary S protein-thrombin-antithrombin III complex. Blood 71:1581–1589.

66. Nishiuchi R, J Takagi, M Hayashi, H Ido, Y Yagi, N Sanzen, T Tsuji, M Yamada and K Sekiguchi. (2006). Ligand-binding specificities of laminin-binding integrins: a comprehensive survey of laminin-integrin interactions using recombinant alpha3beta1, alpha6beta1, alpha7beta1 and alpha6beta4 integrins. Matrix Biol 25:189–197.
67. Rao NC, SH Barsky, VP Terranova and LA Liotta. (1983). Isolation of a tumor cell laminin receptor. Biochem Biophys Res Commun 111:804–808.
68. Nelson J, NV McFerran, G Pivato, E Chambers, C Doherty, D Steele and DJ Timson. (2008). The 67 kDa laminin receptor: structure, function and role in disease. Biosci Rep 28:33–48.
69. Kurosawa H. (2012). Application of Rho-associated protein kinase (ROCK) inhibitor to human pluripotent stem cells. J Bio Bioeng 114:577–581.
70. Watanabe K, M Ueno, D Kamiya, A Nishiyama, M Matsumura, T Wataya, JB Takahashi, S Nishikawa, K Muguruma and Y Sasai. (2007). A ROCK inhibitor permits survival of dissociated human embryonic stem cells. Nature Biotechnol 25:681–686.
71. Heng YW and CG Koh. (2010). Actin cytoskeleton dynamics and the cell division cycle. Int J Biochem Cell Biol 42:1622–1633.
72. Votteler M, PJ Kluger, H Walles and K Schenke-Layland. (2010). Stem cell microenvironments—unveiling the secret of how stem cell fate is defined. Macromol Biosci 10:1302–1315.
73. Brizzi MF, G Tarone and P Defilippi. (2012). Extracellular matrix, integrins, and growth factors as tailors of the stem cell niche. Curr Opin Cell Biol 24:645–651.
74. Peerani R, BM Rao, C Bauwens, T Yin, GA Wood, A Nagy, E Kumacheva and PW Zandstra. (2007). Niche-mediated control of human embryonic stem cell self-renewal and differentiation. EMBO J 26:4744–4755.
75. Davey RE and PW Zandstra. (2006). Spatial organization of embryonic stem cell responsiveness to autocrine gp130 ligands reveals an autoregulatory stem cell niche. Stem Cells 24:2538–2548.
76. Lian X, J Zhang, SM Azarin, K Zhu, LB Hazeltine, X Bao, C Hsiao, TJ Kamp and SP Palecek. (2013). Directed cardiomyocyte differentiation from human pluripotent stem cells by modulating Wnt/beta-catenin signaling under fully defined conditions. Nat Protoc 8:162–175.

Address correspondence to:
Dr. Steve Kah-Weng Oh
Stem Cell Group
Bioprocessing Technology Institute
*Agency for Science, Technology and Research (A*STAR)*
Centros Level 4
20 Biopolis Way
Singapore 138668
Singapore

E-mail: steve_oh@bti.a-star.edu.sg

Dr. William R. Birch
Institute of Materials Research and Engineering
*Agency for Science, Technology and Research (A*STAR)*
3 Research Link
Singapore 117602
Singapore

E-mail: w-birch@imre.a-star.edu.sg

Received for publication December 27, 2013
Accepted after revision March 17, 2014
Prepublished on Liebert Instant Online March 18, 2014